이학석사학위논문

Electrical and Magnetic Control of Nanostructures for the Biochip Applications

나노구조체의 전기적 자기적 조절과 이를 이용한 바이오 칩 분야의 응용에 관한 연구

2014 년 2 월

서울대학교 대학원

생물물리 및 화학생물학과

이 동 준

Electrical and Magnetic Control of Nanostructures for the Biochip Applications

(나노구조체의 전기적 자기적 조절과 이를 이용한 바이오 칩 분야의 응용에 관한 연구)

지도 교수 홍 승 훈

이 논문을 이학석사 학위논문으로 제출함

2014 년 2 월

서울대학교 대학원

생물물리 및 화학생물학과

이 동 준

이동준의 이학석사 학위논문을 인준함

2014 년 2 월

위 원 장 홍 성 철 (인)

부위원장 홍 승 훈 (인)

위 원 석 영 재 (인)

Electrical and Magnetic Control of Nanostructures for the Biochip Applications

Dong Jun Lee

Supervised by

Professor Seunghun Hong

A Dissertation Submitted to the Faculty of

Seoul National University
in Candidacy of the Degree of Master of Philosophy

February 2014

Department of Biophysics and Chemical Biology

Graduate School

Seoul National University

Abstract

Electrical and Magnetic Control of Nanostructures for the Biochip Applications

Dong Jun Lee

Department of Biophysics and Chemical Biology

The Graduate School

Seoul National University

In this dissertation, we report ways to modulate nanostructures using electrical and magnetic stimulation and their possible applications in biochip application.

First, we report the development of “nano-storage wires” (NSWs), which can store chemical species and release them at a desired moment via external electrical stimuli. Here, using the electrodeposition process through an anodized aluminum oxide template, we fabricated multisegmented nanowires composed of a polypyrrole segment containing adenosine triphosphate (ATP) molecules, a ferromagnetic nickel segment, and a conductive gold segment. Upon the application of a negative bias voltage, the NSWs released ATP molecules for the control of motor protein activities. Furthermore, NSWs can be printed onto various substrates including flexible or three-dimensional structured substrates by direct writing or magnetic manipulation strategies to build versatile chemical storage devices. Since our strategy provides a means to store and release

chemical species in a controlled manner, it should open up various applications such as drug delivery systems and biochips for the controlled release of chemicals.

Additionally, we report the development of ultra-fast enzyme-linked immunosorbent assay (ELISA) method through the utilization of magnetic capture and release cycle. Our system is largely consisting of two components; array of primary antibody labeled nickel patterns on the substrate and superparamgnetic nanoparticles functionalized with secondary antibody. Upon the application of cyclic magnetic field, the superparamgnetic nanoparticles are actively captured and released from the nickel patterns. When the superparamagnetic particles captures antigens present in the solution and deliver them to nickel patterns, interaction between the primary antibody-antigen-secondary antibody prevents the superparamgentic particles being released from the nickel patterns during the capture and release cycle. Through this mechanism, it was possible to detect the presence of antigen within 5 minutes. Since our strategy provides a means to reduce the detection time significantly, it should open up various applications such as development of ultra-fast biosensors and cargo delivery in biochips.

Keywords: nanowire, polypyrrole, controlled release, printable, bioenergy storage, nano-bio interface, superparamagnetic nanoparticles, detection time, enzyme-linked immunosorbent assay (ELISA), magnetic capture and release, biochip.

Student Number: 2012-22515

Table of Contents

List of Figures

Chapter 1.

Introduction

1.1 Biochips and Biosensors

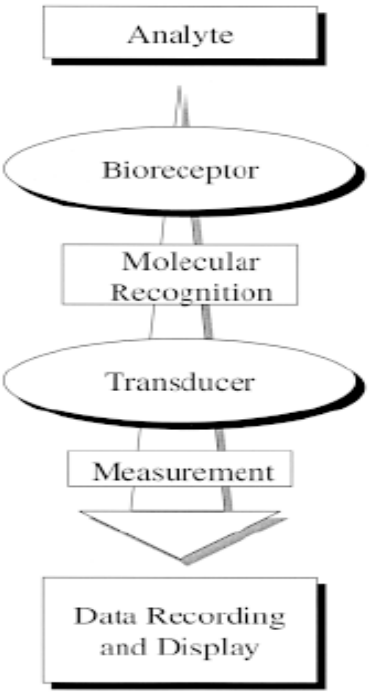

Figure 1.1 Conceptual diagram of the biosensing principle.[1]

For the past few decades, biological and diagnostic field have witnessed great advances in the development of biosensors and biochips which can identify and quantify the target molecules. Conceptually, biosensors can be described as an integrated system of a biological recognition element and a transducer element. The commonly used biological recognition elements are DNA, RNA, antibodies and trans-membrane proteins.[1] Thanks to the unique 3D structure and the arrangement of diverse functional

groups in 3D space of these biomolecules,[2] they are capable of recognizing other chemical species or biomolecules with extreme sensitivity and selectivity which is unparalleled to the man-made machineries.[1] The transducer elements convert the recognition events detected by the upstream biological recognition element into a measurable form of signal. The most common form of transducer techniques involves optical measurements and electrochemical measurements.[3] For example, periplasmic binding proteins, which can recognize the target molecules specifically, are coupled with fluorescent dye. When the recognition events occur, the conformation of the protein changes which affects the local environment of the fluorescent dye. This results in the changes of the fluorescence property which in turn can be measured by an axillary spectrometer.[4] In surface plasmon resonance based biosensors, the binding of target molecules to the receptors causes change in the refractive index at the surface material which provides binding kinetics and concentration of target molecules.[5] In the development of electrochemical sensors for the proteins the gating effect of the field effect transistors (FETs) have been utilized as a means to detect the target protein molecules. For carbon nanotube-FET sensors, the change in the local charge distribution resulted from the proteins binding to the device serves to gate the current flow in the CNT channel.[6]

1.2 Application of Nanostructures in Biochip Applications

Nanotechnology is playing increasingly important role in the development of biosensors and biochips. The utilization of nanomaterials improves the sensitivity and the performance of biosensors.[7] Numbers of different nanostructures such as nanowires and nanoparticles have been employed in field of biosensor and biochip developments. Many researches have studied a means to control the nanostructures. For example, magnetic field was used to control the localization and alignment of ferromagnetic nanowires which allowed fabrication of nanowire based FET transistor.[8] Additionally, ultrasonic wave and electric field was utilized to manipulate the movement of nanowires in the solution.[9] And also, the application of superparamagnetic nanoparticles in biosensing has been extensively studied.[7] In one example, magnetic nanoparticles functionalized with receptor molecules which allowed detection of target molecule through magnetic field-assisted aggregation.[10]

1.3 Motivation

Although there were number of impressive advances in the biochip and biosensor developments, there are some inherent limitations of current biosensor technologies yet to be resolved. The activity of protein molecules is inherently controlled by chemical molecules which act as activation signals or energy sources.[11] For example, biomotors require adenosine triphosphate (ATP) to generate force and motion in living cells.[12] Since the biochips[13,14] and biosensors[15,16] have been relying on

such interactions between proteins and chemical molecules, it is of great importance to develop technologies for the controlled release of signaling chemical molecules in the fabrication of devices relying on protein functionalities. Additionally, there was lot of effort to develop biosensors which can detect very low concentration of the target molecules. However, most of these detection strategies relied on passive diffusion of receptor and target elements for the recognition of each other. Therefore, the time required for the recognition increases dramatically as the concentration of the target decreases.[17] Thus it is of great importance to develop technologies to reduce the detection time in the development of biosensors. Herein, we develop technologies to actively control the biomolecules and transport the chemical and biological molecules through the utilization of electric and magnetic control of nanostructures.

Chapter 2.

Nano-Storage Wires: Electrical and Magnetic Control of Nanowires

2.1 Introduction

The activity of protein molecules is inherently controlled by chemical molecules which act as activation signals or energy sources.[11] For example, biomotors require adenosine triphosphate (ATP) to generate force and motion in living cells.[12] Various applications such as biochips [13,14] and biosensors [15,16] have been relying on such interactions between proteins and chemical molecules. Thus, it is of great importance to develop technologies for the controlled release of signaling chemical molecules in the fabrication of devices relying on protein functionalities. [18-27] For example, the “caged ATP” method utilized UV-active compounds which can hold ATP and release it in the solution upon the exposure to the UV lights. [25-28] Also, various other methods such as conducting polymer-based devices [19-21] and microfluidic devices [22-24] been intensively studied for the controlled release of biochemical molecules. [18] However, these methods often suffered from various limitations. For example, previous methods can be utilized to control the biomolecular concentration over entire solution, but it is often very difficult to control the local concentrations of desired biomolecules.[29-31] And also, many of previous methods required macroscopic auxiliary devices [22, 25-30] such as pumps and UV-light sources which cannot be integrated into compact devices for nanomechanical systems. On the other hand, nanoparticles (NPs) [31-33] or nanowires

(NWs) [34-35] synthesized from the combination of various materials have been applied to drug delivery systems [31-33] or printable electrical devices [36,37] since the NPs and NWs can be guided to the desired locations by external forces.[36-40] However, nanostructures which can store and release specific chemicals upon electrical stimuli have not been developed yet.

Herein, I developed “nano-storage wires” (NSWs) which can store chemical species and release them when stimulated by an external electrical bias. In this work, electrodeposition techniques [38,41] were utilized to fabricate multi-segmented NWs composed of a polypyrrole (PPy) segment containing chemical species such as ATP, a ferromagnetic nickel (Ni) segment, and a conductive gold (Au) segment. Due to the Ni segment, the NSWs could be drove and deposited onto specific regions on electrode surfaces *via* an external magnetic field. [38,39] The NSWs on the electrodes formed a good electrical contact with the electrodes *via* the Au segment, and they released chemical species from the PPy segment[38,42-44] by the external electric potential from the electrodes. As a proof of concept, I demonstrated the control of motor protein activities using NSWs containing ATP. I also showed that NSWs can be printed on flexible or even on 3D structured substrates to build chemical storage devices. Since the NSWs can store chemical species and release them at any desired moment *via* external stimuli, they can be utilized for various biochip applications such as the controlled delivery of drugs and other chemicals for the control of protein activities. [42]

2.2 Experimental Procedures

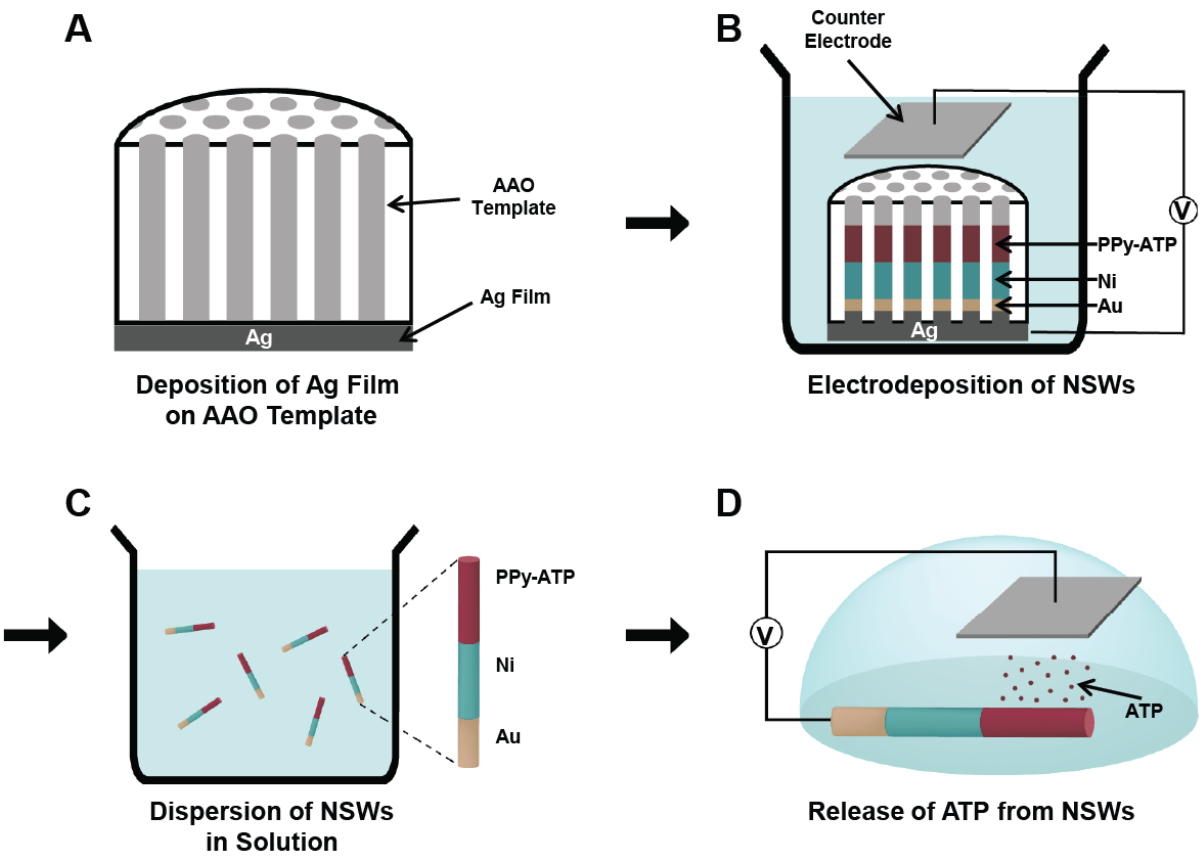

Figure 2.1 Schematic diagram depicting the fabrication of NSWs. (a) Deposition of Ag onto an AAO template. 500 nm-thick Ag layer was thermally evaporated onto the one side of the AAO template to serve as a working electrode. (b) Electrodepostion processes of NSWs. The Au, Ni and PPy-ATP were electrochemically deposited in series. *Yellow*, *blue* and *red* segments represent *Au*, *Ni* and *PPy-ATP* segments, respectively. (c) Dispersion of NSWs into the solution. The *Ag layer* and the *AAO template* were removed by *nitric acid* and *3 M NaOH*, respectively. (d)

Controlled release of ATP from a NSW by applying a negative bias voltage onto the NSW. The bias voltage of -2 V was applied to the NSWs to release ATP molecules in a controlled manner.

Figure 2.1 displays process to fabricate NSWs and perform controlled release of ATP molecules. For the fabrication of NSWs, an anodic aluminum oxide (AAO, Anodisc, Whatman Inc., USA) membrane was used as a template. The *pore size* and the *thickness* of the AAO template were *200 nm* and *60 μm*, respectively. First, a 500 nm-thick Ag layer was thermally evaporated onto the one side of the AAO template.[41,45] Then, the AAO template was installed on a custom built Teflon electrochemical cell (diameter of 8 mm) and immersed in Ag plating solution (Techni Silver 1025, Technic Inc., USA). An additional Ag layer was electrochemically deposited using a potentiostat (Reference 600, Gamry Instruments Inc., USA) at the bias voltage of -0.9 V. In this process, a platinum (Pt) wire with 1 mm diameter (I-Nexus Inc., Korea) was used as a counter electrode, and an Ag/AgCl electrode (MF-2052, Bioanalytical System Inc., USA) was used as a reference electrode. The desired Au (Orotemp 24, Technic Inc., USA) and Ni (High Speed Nickel Sulfamate FFT, Technic Inc., USA) segments were sequentially deposited at the bias voltage of -0.9 V. Finally, PPy-ATP segments were deposited using pyrrole-ATP deposition solution (0.1 M pyrrole (Sigma Aldrich, USA) and 20 mM ATP (Sigma Aldrich, USA)) at the bias voltage of +0.9 V. After the completion of each deposition process, the electrochemical cell was thoroughly rinsed using deionized water. After all the electrodeposition processes, the Ag backing layer was removed using 70 % nitric acid (Sigma Aldrich, USA), and then the AAO template was dissolved in 3 M NaOH solution to disperse NSWs. The dispersed NSWs were centrifuged, and the supernatant was

replaced with deionized water at least three times.

To characterize the NSWs, a field emission scanning electron microscope (FE-SEM) (Hitachi 4800, Hitachi, Japan) was used for the imaging of NSWs. The composition of the each segment of the NSWs was analyzed by an energy dispersive X-ray spectroscopy (EDS) (Hitachi 4800, Hitachi, Japan).

The NSWs were deposited onto a specific location on a solid substrate using ferromagnetic Ni patterns. First, the photoresist (AZ 5214) was patterned on a cover glass *via* the conventional photolithography process, followed by the thermal evaporation of Ni (200 nm). Subsequently, the photoresist pattern was removed by immersing the substrate in acetone. Finally, the NSW solution was placed on to the Ni patterns, and an external magnetic field (50 mT) was applied in the perpendicular direction to the plane of the substrate using a solenoid until the solution was dried.

For the ATP bioluminescence assay, the solution containing the NSWs was placed on a desired substrate (*i.e.*, a Ti/Au (10/30 nm) coated glass slide), and the substrate was subjected to a vacuum chamber for 1 h to dry out the solution. The flow cell was constructed by covering the deposited substrate with a Ti/Au (10/30 nm) coated glass slide as a counter electrode and the 3M double-sided tapes was used as a spacer. The ATP bioluminescence assay solution (Sigma Aldrich, USA) was prepared as recommended in the provider's manual. The assay solution was injected into the flow cell, and the negative bias voltage of -2 V was repeatedly applied for the release of ATP from the NSWs. The luminescence from the reaction was observed *via* fluorescence

microscopy (TE2000U, Nikon, Japan) at a FITC channel (EX 540/25, DM 565, BA605/55, Nikon, Japan).

For the *in-vitro* motility assay of kinesin, NSWs were deposited on a Ti/Au (10/30 nm) coated glass substrate, and then a flow cell was fabricated. Afterwards, the flow cell was incubated with casein solution (0.5 mg mL^{-1} in BRB80 buffer) for 3 min. Then, it was incubated with bacterially expressed kinesin solution (0.2 mg mL^{-1} kinesin, 0.5 mg mL^{-1} casein in BRB80 buffer) for 30 min. Microtubule solution containing rhodamine-labeled microtubules (0.1 μM tubulin), 20 μM Taxol, 1 mM dithiothreitol (DTT), anti-bleaching cocktail (3 mg mL^{-1} D-glucose, 0.1 mg mL^{-1} glucose oxidase, 0.017 mg mL^{-1} catalase) and a redox mediator (3 mM ferrocene-dimethanol ($Fc(MeOH)_2$)) in BRB80 buffer was introduced to the flow cell, and the flow cell was incubated for 3 min. Since the motility of the microtubule-kinesin system is temperature sensitive[46], the temperature was maintained at 35°C using a microscope incubation system (INU-TIZ-F1, Tokai Hit, Japan).

For the fabrication of Single NSW-based devices, Ni/Au (200/30 nm) electrodes were fabricated first *via* the conventional photolithography process. [38] Then, the NSW solution was dropped on the Ni/Au electrodes. Finally, a magnetic field (50 mT) was applied in the perpendicular direction to the long axis of the linear Ni/Au electrodes in order to localize the individual NSW on top of two neighboring Ni/Au electrodes separated by 5 μm.

For the Direct Writing of NSWs, Commercially available Ni-needles were

magnetized inside a solenoid (50 mT) and dipped into the NSW solution (10^{10} unit mL^{-1}) so that a small droplet of the NSW solution was formed at its end. Then, the needle was installed on a probe-manipulator (MST-PM50, MS Tech., Korea) and utilized as a *pen* to directly write NSWs on a Ti/Au (10/30 nm) coated glass substrate.

For the Fabrication of Flexible Devices, A commercially available Kapton polyimide film (0.2 mm, DuPont Inc, USA) was sonicated in acetone and then used to fabricate a flexible device. For the formation of a working electrode, Ti/Au (10/30 nm) layers were thermally deposited on the polyimide film. Subsequently, Ni line patterns with 100 nm thickness were fabricated on the top of the Ti/Au coated polyimide film. NSW solution (10^{10} unit mL^{-1}) was dropped on the polyimide film, while a magnetic field (50 mT) was applied along the long axis of the Ni line patterns.

For the fabrication of probe-type storage device, Borosilicate glass capillaries with an initial inner diameter of 1.2 mm and outer diameter of 1.5 mm (World Precision Instruments Inc., USA) were used as starting materials for the fabrication of micropipettes. A glass capillary was loaded on a vertical micropipette puller (PC-10, Nari shige, Japan). The center of the glass capillary was pre-heated by applying 68 V and post-heated by applying 48 V to the heater element of the puller. Then, the capillary was stretched to cut. After pulling the capillary, the surfaces of the micropipette was treated with Piranha solution (H_2SO_4 : H_2O_2 = 4:1). [47] The entire surface of the micropipette was covered with Ti/Au (10/30 nm) layers through several thermal evaporation process. Finally, the tip of the micropipette was dipped into the NSW solution (10^{10} unit mL^{-1}) for

5 minutes so that NSWs adhere onto it.

2.3 Characterization of Nano-Storage Wires

Each segment of the NSWs was designed to carry out specific functions. The PPy-ATP segment has been utilized for the controlled release of ATP molecules. [19-21] The Ni segment enables the magnetic localization of NSWs, [38,39] while the Au segment provides a good electrical contact with electrodes. When Ni is exposed to air or aqueous condition, the surface oxidation results in high contact resistance.[48,49] Therefore, the Au segment was incorporated to lower the contact resistance between the NSWs and the electrodes.[50] The detailed procedure for the NSW fabrication method can be found in the Materials and Methods section. In brief, 500 nm-thick silver (Ag) layer was thermally evaporated on one side of an anodized aluminum oxide (AAO) template (Figure 1a) to serve as a working electrode. [41] After the thermal deposition of an Ag layer, additional Ag was electrochemically deposited using a potentiostat to create a uniform working electrode for the deposition of NSWs. [45] The desired Au, Ni, and PPy-ATP segments were deposited in series (Figure 1b). Following the deposition, the Ag backing layer was etched using 70 % nitric acid,[51] and then the AAO was dissolved in 3 M NaOH solution [40] to disperse the NSWs in the solution (Figure 1c). Here, only the Ag layer deposited on the side of the AAO template was exposed to the nitric acid, and the Au segment prevents the intrusion of the nitric acid to the Ni and PPy segments. It prevented potential damages to the ATP stored in the PPy parts. Furthermore, since the diffusion of small ions such as NaOH in the solution towards the core of the PPy matrix

is negligible, [52,53] the most of ATP molecules can be stored stably within the PPy segment. The dispersed NSWs were thoroughly rinsed with deionized water prior to the release experiments. Figure 1d shows a schematic diagram depicting the measurement of the real-time controlled release of ATP from a NSW. Here, the NSW as well as a counter electrode was placed in the solution of ATP bioluminescence assay kit containing luciferin and luciferase. When the negative bias voltage of -2 V was applied to the NSW, the PPy-ATP segment in the NSW expanded and released ATP. Due to the released ATP, the luciferin around the NSW was rapidly oxidized by luciferase, producing light. Thus, the observation of such light around the NSW by fluorescence microscopy can be an

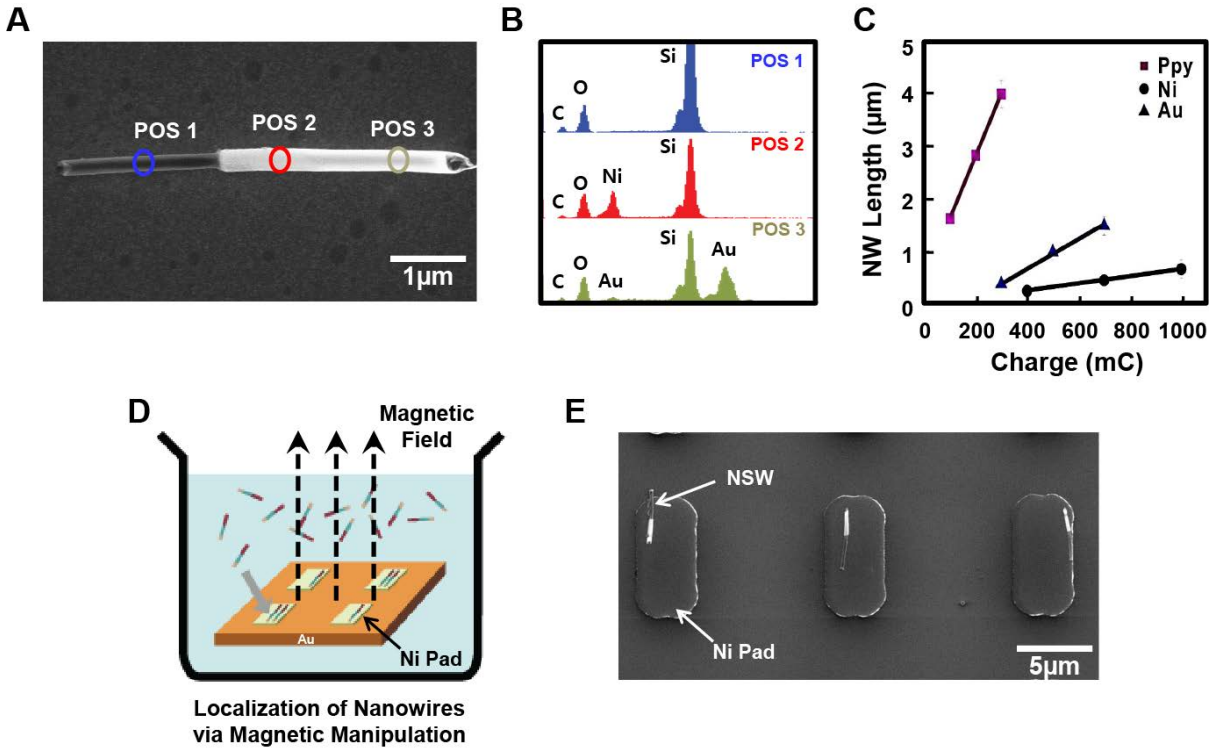

indication of the ATP release from the NSW.[34]

Figure 2.2 Characterizations of NSWs. (a) SEM image of a single NSW. The *dark*, *intermediate* and *bright* regions represent *PPy-ATP*, *Ni* and *Au* segments, respectively. (b) EDS spectra on the NSW. The *blue*, *red*, and *green* spectra correspond to position *1*, *2* and *3* of the Figure 2a, respectively. (c) Growth length of each segment *versus* applied charges. (d) Schematic diagram depicting the localization of NSWs driven by magnetic fields. NSWs in the solution were attracted to pre-defined Ni patterns when external magnetic fields were applied. (e) SEM image of NSWs localized on Ni patterns.

Figure 2.2a shows the scanning electron microscopy (SEM) image of NSWs. The NSW consisted of three distinct segments; *dark*, *intermediate*, and *bright* regions corresponding to *PPy-ATP*, *Ni* and *Au* segments, respectively. To confirm the chemical compositions of each segment, we performed the energy dispersive X-ray spectroscopy (EDS) (Figure 2.2b). Position *1* (POS1) of the NSW mainly consisted of carbon and oxygen, whilst Positions *2* (POS2) and *3* (POS3) contained *Ni* and *Au*, respectively. Strong Si peaks appeared in all regions since the NSWs were loaded onto a silicon oxide wafer for the EDS analysis. These EDS results clearly confirmed that our fabrication method allowed the synthesis of NSWs with discrete segments.

Figure 2.2c shows the length of each segment with respect to applied charges during electrodeposition. The EDS analysis in the line scanning mode was conducted along the long axis of NSWs to investigate the precise lengths of each segment. The length of the each segment linearly correlated with the applied charges. The growth rate

was 14 nm/mC for the PPy-ATP segment, 0.9 nm/mC for the Ni segment, and 3.2 nm/mC for the Au segment (Figure 2.2c). This result implies that it is possible to control the length of each segment simply by controlling the applied charges during the electrodeposition process.

Each segment in a NSW plays a role to extend the applications of the NSWs. The PPy segment stores chemical species such as ATP. The Au segment enables a good electrical contact between the deposited NSWs and the electrodes because Au does not form an insulating oxide layer on it. The Ni segment of the NSWs allows one to utilize magnetic fields to drive the NSWs and place them onto a specific location for device applications. As a proof of concept, I demonstrated the deposition of NSWs onto a specific location on a solid substrate using ferromagnetic Ni patterns (Figure 2.2d).[38] Here, Ni patterns (5 μm × 10 μm) on a silicon oxide wafer were placed in the dispersions of NSWs, and an external magnetic field was applied. In this case, the magnetic field around the Ni patterns became larger than other regions, and, thus, the NSWs were driven to the Ni patterns due to its magnetic segment. Figure 2.2e shows the SEM image of NSWs on ferromagnetic Ni-patterns. The NSWs were aligned and localized on the Ni-patterns. This result indicated that the position and the alignment of individual NSW can be controlled by utilizing magnetic fields, which can be utilized to assemble complicated device structures for practical applications.

2.4 Controlling the Release of ATP and the Biomotor Activity *via* Electrical Stimuli

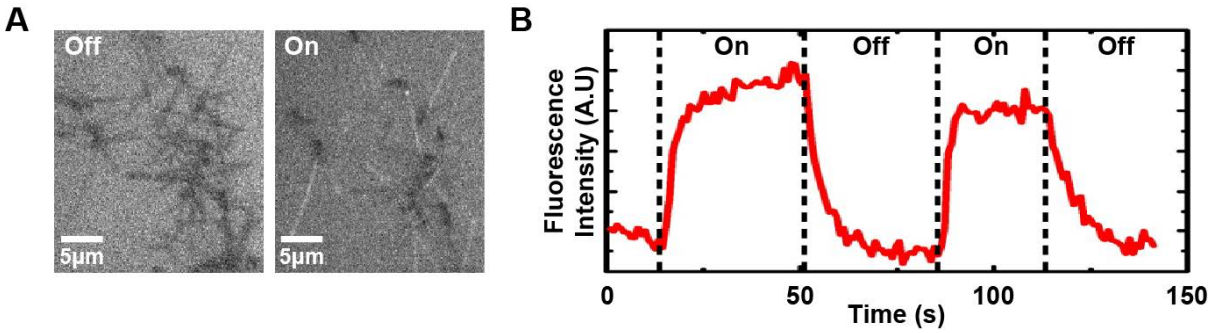

Figure 2.3 Controlled release of ATP *via* electrical stimuli. (a) Fluorescence images of NSWs on Au substrate with (left panel) and without (right panel) the application of -2 V bias voltage. The ATP bioluminescence assay kit (luciferin/luciferase kit from Sigma Aldrich, USA) was used to detect the release of ATP. (b) Graph of the fluorescence intensity with respect to time. The fluorescence intensity indicating ATP molecules was repeatedly *increased* and *decreased* with *application* and *removal* of -2 V bias voltage, respectively. The data were obtained from the NSWs in (a).

Figure 2.3a shows fluorescence micrographs of NSWs with (left panel) and without (right panel) the application of bias voltages as described in Figure 2.1d. Without a bias voltage, NSWs appeared as dark regions (left panel). When a negative bias voltage was applied, the PPy-ATP segments expanded and released ATP into the solution. The released ATP stimulated the oxidation of luciferin around the NSW, producing lights (right panel). Note that although the released ATP could usually diffuse out over a long

distance in solution environments, [42] in this experiment, it reacted with nearby luciferase and luciferin immediately and generated fluorescence light only near the NSWs. This result clearly shows that our NSWs could store biochemical species such as ATP and release them by electrical stimuli. It also should be noted that the Au segments without oxide layers should have helped making a good electrical contact with the electrode surfaces. We performed a control experiment using a conducting AFM to estimate the effect of Au segments on the contact resistance of NSWs. The results show that the NSWs with Au segments had 600 times or lower contact resistance than those without Au segments.

Figure 2.3b displays the fluorescence intensity of the NSWs as a function of time. The fluorescence intensity was averaged over the NSWs as shown in Figure 3a. The fluorescence intensity increased with the application of -2 V bias voltages, but it decreased abruptly with the removal of the bias voltages. The fluorescence intensity of NSWs confirmed that the PPy-ATP segment released ATP molecules when the bias voltage was applied, while it ceased to release when the bias voltage was removed. It should be noted that, upon the application of electrical stimuli, ATP molecules could be repeatedly released from the NSWs with a short response time.

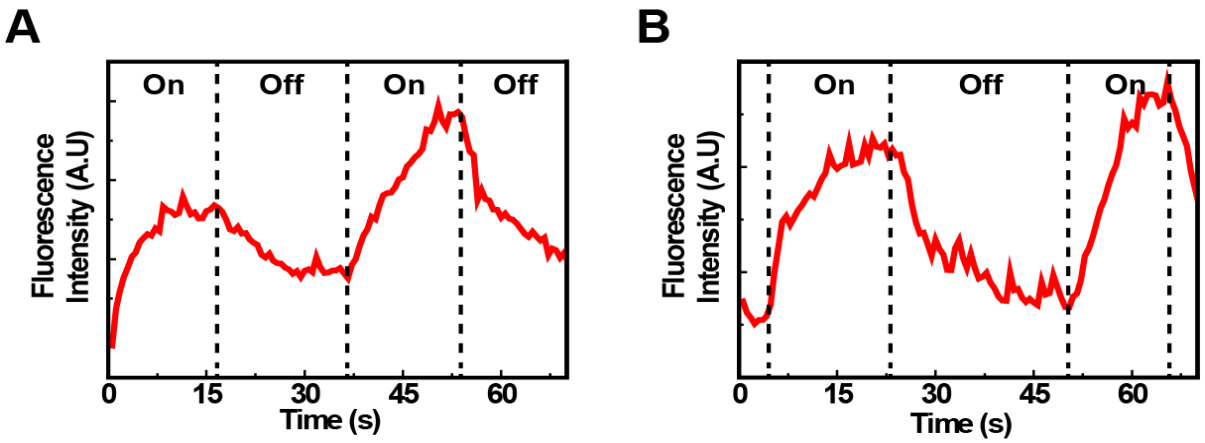

Figure 2.4 Activation of NSWs after long term storage. (a) ATP bioluminescence assay Intensity from the deposited NSWs after 12 hour storage in dry condition. Here, NSWs were deposited on the Au substrate like in Figure 3a and stored in a dry condition for 12 hours. Then, the sample was placed in the bioluminescence assay and the bias voltage of -2V was applied to the NSWs. The results indicate the repeated release of ATP. (b) ATP bioluminescence assay Intensity from NSWs after the NSWs were stored in DI water at -20 °C for 2 weeks in prior to the deposition.

It is also worth discussing the lifetime of the chemical species in NSWs. The lifetime of NSWs is expected to vary depending on the properties of stored chemical species and environmental conditions. In case of ATP, it can be easily destroyed when moisture in the PPy segment is completely removed. We could keep the deposited NSWs under dry environments over 12 hours and demonstrate the release of ATP (Figure 2.4a). However, we can expect that for a longer storage of ATP in the NSWs, the device should be stored in humid or wet environments. The ATP in NSWs is expected to be stored for a long time period at a low temperature just like other biological molecules. For example,

we could store the NSWs with ATP in the deionized water at -20 °C for 2 weeks and use them to release ATP (Figure 2.4b).

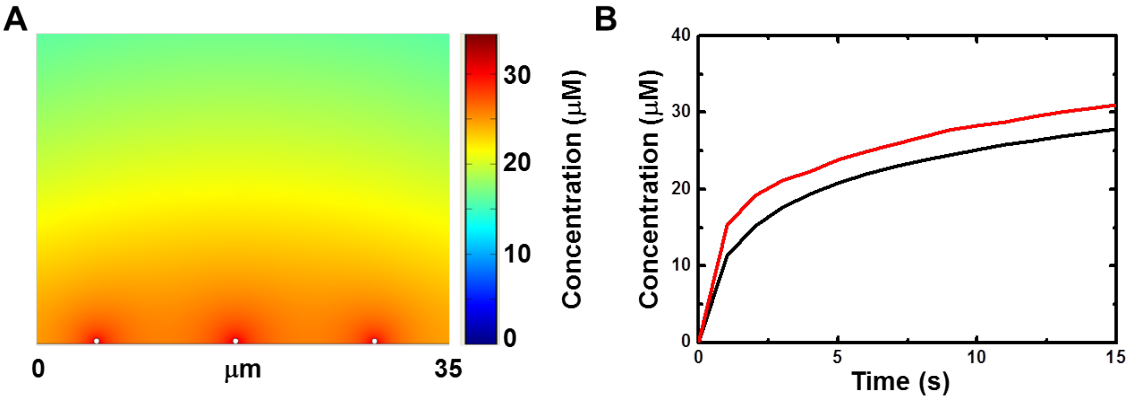

Figure 2.5 Simulation results of ATP release from the NSWs. (a) Concentration of ATP released from deposited NSWs after electrical stimuli for 10s. The simulation was performed as described in Supplementary Note 1. (b) Graph of ATP concentration with respect to time. The *red* and *black* lines indicated the ATP concentration *at the vicinity of the NSWs* and *at 5 μm away from the NSWs*, respectively.

We performed a simulation to estimate how much ATP can be stored in each NSW and can be released from it (Figure 2.5). In brief, the initial ATP concentration within a NSW was estimated as 0.81 M considering the dimension of NSWs and the concentration of the used chemical species. Then, the ATP release from the NSWs was simulated using a commercial finite element method package, COMSOL Multiphysics. We modeled our NSW system based on the thin layer diffusion model. [42,54] On the basis of the simulation result, ATP concentration inside the PPy-ATP segment was estimated to be 0.81 M at 0 s, 0.60 M at 5 s and 0.40 M at 10 s during the application of a

negative bias voltage (Figure 2.5). Therefore, 12 x 10^{-17} mol of ATP was released from each NSW for each 10 s at the initial stages. Assuming that the ATP in our present PPy-ATP patterns was used up to fill our flow cell with its dimension of 1 cm x 0.8 cm x 150 μm (W x L x H), the ATP concentration in the flow cell could increase up to 119.85 μM. However, it also should be noted that the maximum possible ATP concentration by our method can be increased much further simply by depositing more NSWs, implying that our method can be utilized to control the ATP concentration from zero up to a very high concentration.

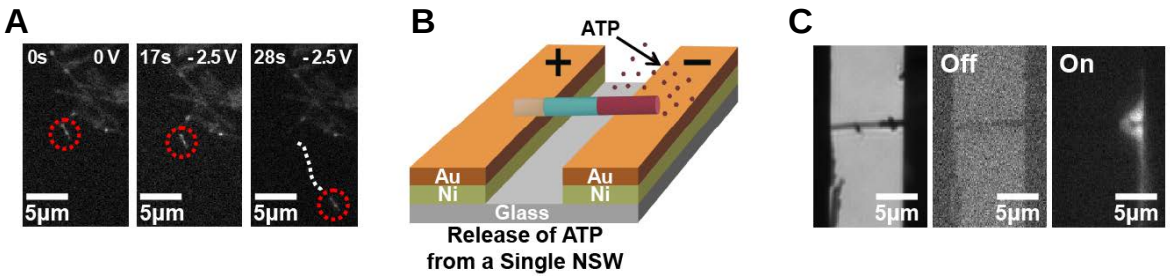

Figure 2.6 Control of biomotor motility using NSWs and controlled release of ATP from single NSW device. (a) Control of biomotor motility using NSWs. Here, the thin Au surface on glass was coated with kinesin biomotors. The white line in the red dotted circle represents a microtubule on the kinesin biomotors. Other white lines represent the NSWs on the substrate. (b) Schematic diagram depicting the controlled release of ATP from an individual NSW between two electrodes. The NSW was magnetically localized onto an electrode consisting of Ni (green) and Au (orange), and then -2 V bias voltage was applied across the NSWs. (c) Optical (left) and fluorescence image of a single NSW with (middle) and without (right) -2 V bias voltage.

The released ATP could be utilized to control the activities of protein molecules such as biomotors (Figure 2.6a). Here, NSWs were first deposited onto a thin Au film,

and, then, the Au film was utilized as a substrate for the microtubule-kinesin motility assay. [47] When a bias voltage was applied onto the substrate, ATP was released from the NSWs. The kinesin molecules were activated, resulting in the motion of microtubules on them. [42] It is worth discussing the advantages and disadvantages of our method for the control of biomotor activities compared with previous works. Previously, a thermoelectric chip has been utilized to control the localized activity of biomotors by controlling the local temperature. [55-57] This method can efficiently turn on and off all biomolecular activities related with temperature in a localized region. However, in our method, one can selectively control the biomolecular activities related with ATP or any released chemical species while leaving other biomolecular activities unaltered. Thus, our NSWs should be a new powerful tool for the selectively control of specific biomolecular activities in a localized region. [28-30,55-57]

We could place individual NSWs between two electrodes for the controlled release of ATP molecules (Figure 2.6b). Here, an external magnetic field was applied to trap a NSW between two Ni/Au electrode patterns from its solution. Figure 2.6c illustrates the optical and the fluorescence images of a single NSW deposited on the top of two neighboring Ni/Au electrodes. The NSW was located on the top of the Ni/Au two neighboring electrodes as expected (left panel). The fluorescence micrograph shows that the NSW luminesced only upon the application of -2 V bias voltage (middle and right panels). In this case, since the bias voltage was applied between two nearby electrodes, an additional separate electrode was not required. Thus, we should be able to fabricate

micro- and even nanoscale storage devices based on NSWs for the controlled release of chemical species. This result also clearly shows that our device can be utilized to control the local concentration of biomolecules without any bulky equipment, which can be an advantage compared with previous methods.[18-27]

2.5 Printable "Nano-Storage" Devices

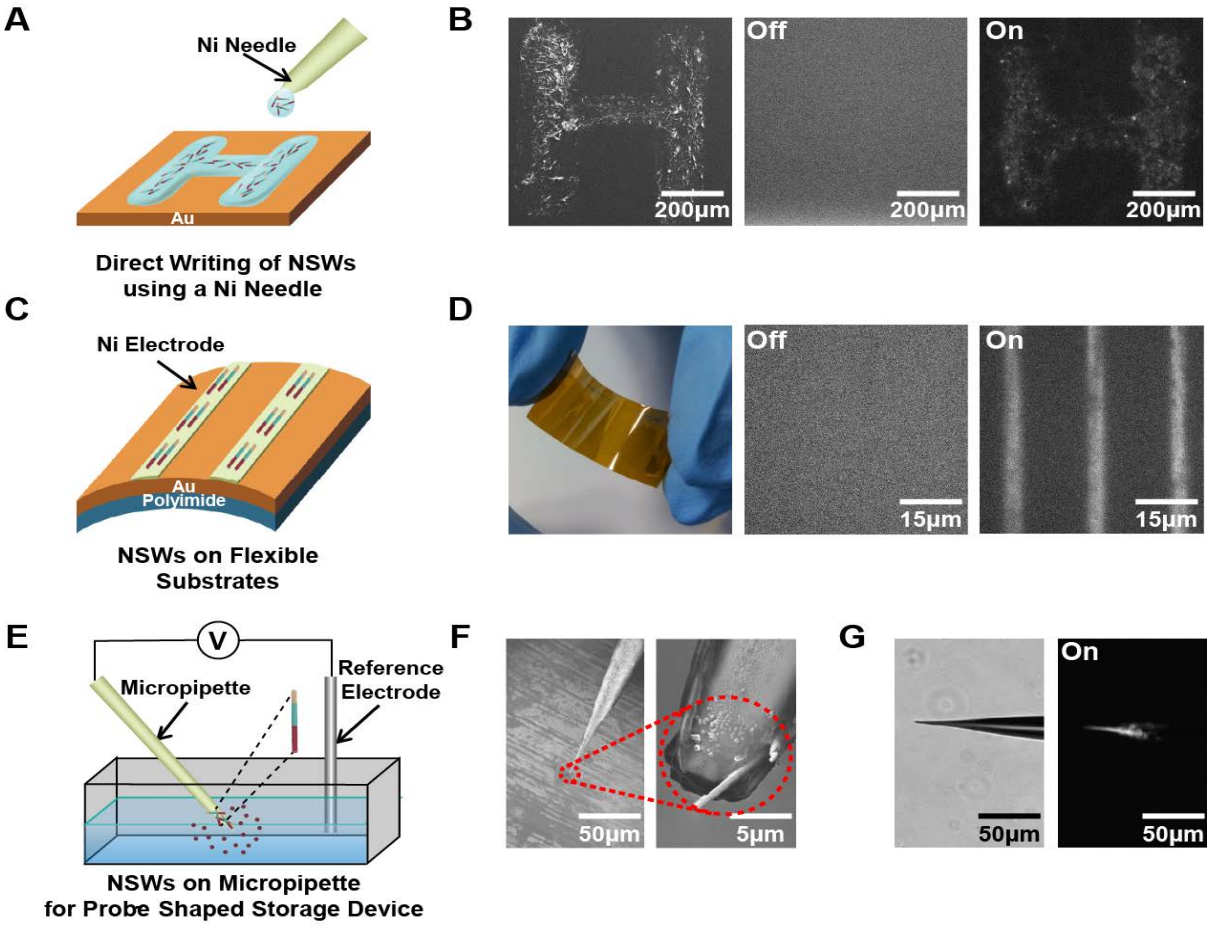

Figure 2.7 Printable "nano-storage" devices. (a) Schematic diagram depicting the direct writing of NSWs onto a solid substrate. 'NSW ink' was written onto Au substrate using a

magnetized needle. (b) SEM image (left) of NSWs printed *via* direct writing and fluorescence image of the same sample with (right) and without (middle) the application of -2 V bias voltages. The ATP bioluminescence assay solution (luciferin/luciferase kit from Sigma Aldrich, USA) was used to detect the release of ATP. (c) Schematic diagram showing a flexible nano-storage device. Polyimide film was coated with Au layer and Ni patterns (green). NSWs were driven and deposited on the Ni electrodes *via* external magnetic fields. (d) Photographic image (left) and fluorescence image of the flexible storage device with (right) and without (middle) the bias voltage of -2 V. (e) Schematic diagram depicting the controlled release of ATP from NSWs deposited on a micropipette. The micropipette was placed in the ATP bioluminescence kit, and then the bias voltage of -2 V was applied to release the ATP from the NSWs. (f) SEM image of NSWs deposited on a micropipette. (g) Optical (left) and fluorescence (right) images of NSWs attached on micropipette when the bias voltage of -2 V was applied.

NSWs are quite versatile nanostructures which can be utilized for various chemical storage device applications for controlled release of biochemical species (Figure 2.7). At first, we demonstrated the direct writing of NSWs on solid substrates for a printable device (Figure 2.7a). Here, a Ni needle was dipped into the NSW solution to form a small droplet of 'NSW ink' at its end. Then, it was fixed on a probe-manipulator and used as a 'pen' to directly write NSWs on the Au substrate. Figure 2.7b shows the SEM image (left panel) and fluorescence micrographs (middle and right panel) of NSWs prepared by this direct writing method. The SEM image shows that NSWs are deposited on the substrate in shape of an 'H'. Furthermore, the 'H' shape lit up when the negative bias voltage of -2 V was applied to the underlying Au substrate. It clearly shows that NSWs can be easily written onto the desired region of the substrate to build storage

device structures for the controlled release of biochemical molecules.

We also demonstrated the *flexible* nano-storage devices (Figure 2.7c). Here, NSWs were driven by magnetic fields and deposited onto Ni/Au films on a transparent and flexible polyimide film (left panel of Figure 2.7d). The device transmitted some light, and it can be easily bent. The *middle* and *right* panels of Figure 2.7d are the fluorescence images of flexible nano-storage device *without* and *with* a -2 V bias voltage on the substrate, respectively. Note that the linear patterns containing NSWs illuminated brightly when a negative bias voltage was applied. Since the networks of NSWs are flexible and can be prepared on virtually-general substrates including flexible substrates, it should open up various applications such as flexible storage devices for the controlled release of biochemical molecules.

The NSWs can be deposited onto *curved* surfaces such as sharp end of a micropipette to fabricate quite versatile storage devices (Figure 2.7e). Here, the end of an Au-coated micropipette [58] was placed in the solution of NSWs so that NSWs adhered onto it, resulting in probe-shaped storage devices. Figure 2.7f shows the SEM images of NSWs at the end of the micropipette. When a negative bias voltage was applied to the micropipette, the tip region appeared bright (Figure 2.7g). These results indicate that the release of ATP molecules was localized at the tip of the micropipette where the NSWs were attached. Therefore, such probe-shaped storage devices can be used for the delivery of chemicals to individual cells through a direct injection. And also, these results show that we can deposit NSWs onto virtually any structures to create nanoscale devices for

the controlled release of biochemical materials.

2.6 Summary

In conclusion, we report a NSW structure which can be deposited onto virtually-general substrates to build nano-storage devices for the real-time controlled release of biochemical molecules upon the application of electrical stimuli. The NSWs were three different segments comprised of *PPy*, *ferromagnetic Ni*, and *conductive Au*, each of which was used to *store chemical species*, *align NSWs by magnetic fields*, and *make a good electrical contact to external electrodes*, respectively. NSWs have been deposited onto specific locations on solid substrates *via* various methods such as direct writing or magnetic field driven assembly, and they were utilized for the controlled release of ATP. We also demonstrated the deposition of NSWs onto *flexible substrates* or *the end of micropipettes* to fabricate *flexible* or *probe-type* nano-storage devices, respectively. These results clearly show that NSWs are quite versatile structures allowing us to fabricate nano-storage devices on virtually general substrates for the controlled release of biochemical molecules. Thus, our strategy should provide great opportunities in various areas such as drug delivery systems, [18-21] biosensors [15,16] and biochips [13] for the controlled release of chemicals to bio-systems

Chapter 3.

Enhancing the Response of ELISA Assay using Magnetic Capture and Release Cycle: Magnetic Control of Magnetic nanoparticles

3.1 Introduction

The number of protein molecules inherently possesses ability to recognize other biomolecules such as DNA, proteins and small chemical species. [1] For example, antibodies can recognize and form interaction with target antigen molecules through the geometric and electrostatic complementarity. [2] Various applications such as biosensors and enzyme-linked immunosorbent assay (ELISA) have been relying on such interactions between proteins and other biomolecules in order to detect the presence of target molecules. [1] Numbers of methods have been developed to detect the target molecules at very low concentrations. However, most of these detection strategies rely on passive diffusion of receptor and target elements for the recognition of each other. [5,6] Therefore, the time required for the recognition increases dramatically as the concentration of the target decreases. Thus it is of great importance to develop technologies to reduce the detection time in the development of biosensors. [17] For example, target molecules such as nucleic acid and proteins can be actively guided toward the sensor element through the

utilization of electrostatic fields. [59] Additionally, “magnetic field-assisted aggregation of magnetic particles” utilized magnetic field to aggregate magnetic nanoparticles that have captured target antigens. [10] However, these methods often suffered from various limitations. For example, when electric field is applied to actively transport the biomolecules to the sensor, target biomolecules may be damaged by the external electric field. In the case of “magnetic field-assisted aggregation of magnetic particle” method, the antigens were actively brought to the antibodies. However, this method relied on passive diffusion of magnetic nanoparticles before the additional cycle of sensing which limits the detection time. Therefore, strategies that can actively capture and release the target molecule in cyclic manner, to reduce the detection time, have not been developed yet.

Herein, we report the development of ultra-fast enzyme-linked immunosorbent assay (ELISA) method through the utilization of magnetic capture and release cycle. Our system is largely consisting of two components; superparamagnetic particles functionalized with secondary antibodies and the Ni patterns functionalized with primary antibodies. Upon the application of cyclic magnetic field, the superparamgnetic nanoparticles were actively captured and released from the nickel patterns. When the superparamagnetic particles captures the target antigens floating in the solution and deliver them to nickel patterns, the primary antibody on the Ni pattern forms antigen-antibody interaction which immobilizes the magnetic nanoparticles. Therefore, the fluorescent magnetic nanoparticles accumulate on the Ni patterns during the magnetic capture and release cycle. Through this mechanism, it was possible to detect the presence

of antigen within 5 minute. Since our strategy provides a means to reduce the detection time significantly, it should open up various applications such as development of ultra-fast biosensors and cargo delivery in biochips.

3.2 Experimental Procedure

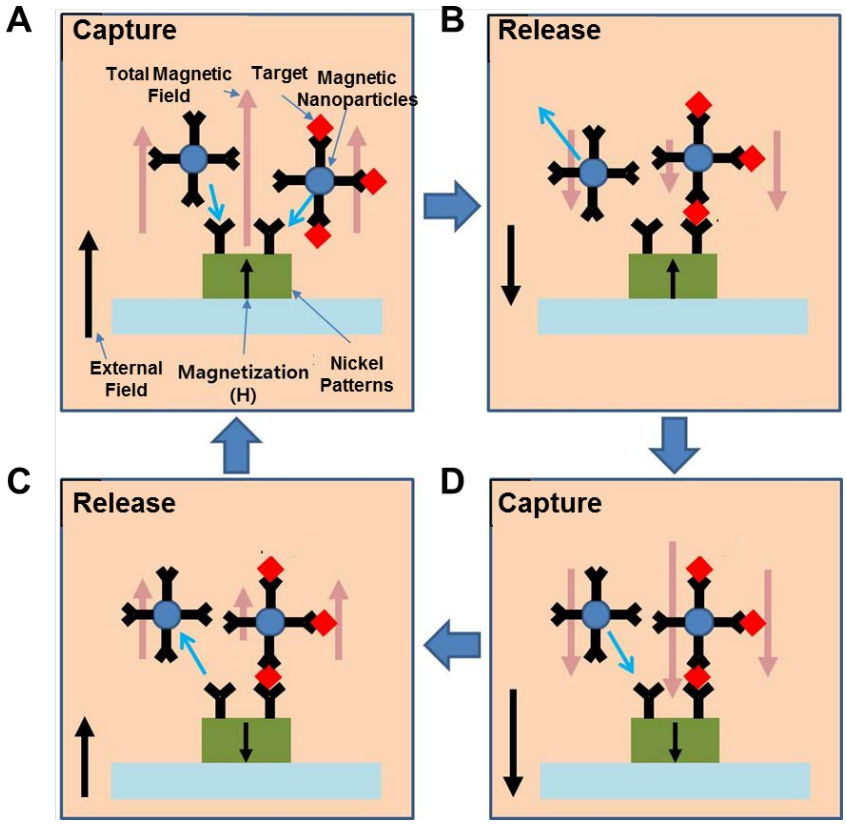

Figure 3.1 Schematic diagram depicting the capture and release cycle. (a) Capture cycle. When external magnetic field is applied in perpendicular direction to the plane of substrate, the magnetic nanoparticles are drawn toward the Ni patterned region. (b) Release cycle. When

external magnetic field was increased in opposite direction while the direction of the local magnetic moment of the Ni patterns remained unchanged, the magnetic nanoparticles were drawn toward the region without the Ni patterns. (c) Capture cycle. The local magnetic fields of Ni patterns eventually aligned with the external magnetic field and the magnetic nanoparticles were drawn toward the Ni patterns. (d) Release cycle. When the external magnetic field was increased in opposite direction while the direction of the local magnetic moment of the Ni patterns remained unchanged, the magnetic nanoparticles were drawn toward the region without the Ni patterns.

Figure 3.1 displays the experimental setup of a magnetic capture and release cycle and their application in the ELISA assay to enhance the response time. First, nickel patterns (5 mm ×10mm) were fabricated on a silicon oxide substrate using conventional photolithographic method. Subsequently, the photoresist patterns were removed by immersing the substrate in acetone. Afterward, the entire surface of the substrate was deposited with additional layer of silicon oxide (50 nm) to minimize the nonspecific binding of biomolecules and magnetic nanoparticles.

For the functionalization of the substrate with antibodies, the substrate was subjected to a commonly used silanization technique. [60] First, the substrate was incubate in 2% solution of 3-mercaptpropyltrimethoxysilane (MTS) in anhydrous toluene for 2 h. The substrate was removed, thoroughly washed with anhydrous toluene and allowed to dry at room temperature. To functionalize the silanized substrate with heterobifunctional linker molecules, the organic hetrobifunctional crosslinker molecule (N-γ–maleimido-butyryloxy succinimide ester (GMBS)) was dissolved in 100 µl of dimethylformamide (DMF) and then diluted with absolute ethanol to a final

concentration of 2mM. The silanized substrate was immersed in cross-linker solution for 1 h and washed three times with PBS buffer. Afterward, 0.15 mg/ml solution of Anti-human IL-13 antibody (Ready-set-go IL-3 ELISA Kit, ebioscience, USA) in PBS buffer was placed on the substrate and allowed to react for 2 h at room temperature. The residual unreacted antibodies were washed with PBS buffer. Finally, the substrate was immersed in the 1% solution of bovine serum albumin (BSA) in PBS for 2 h to passivate the antibody–free regions. [61]

For the functionalization of the superparamagnetic nanoparticles with antibody, commercially available 100 nm sized nanoparticles (1 mg/ml) (nano-screenMAG-Streptavidin, Chemicell, Germany) composed of a magnetite (Fe_3O_4) core, a fluorescent shell and coating coupled with streptavidin was incubated with 1.13 mg/ml solution of anti-human IL-13 antibody (Ready-set-go IL-3 ELISA Kit, ebioscience, USA) labeled with biotin for 1 h at room temperature.

For the repeated magnetic capture and release ELISA assay, the flow cell was constructed by covering the antibody labeled substrate with glass slide and the 3M double sided tape was used as a spacer. Then, the antibody-labeled superparamagnetic nanoparticles (1.8×10^{13} unit/ml) mixed with target antigen (human IL-13 recombinant protein, ebioscience, USA) was injected into the flow cell and placed on top of custom-built solenoid. During the capture cycle, the external magnetic field (150 mT) was applied in perpendicular direction to the plane of the substrate for 30s to draw the magnetic particles toward the Ni patterns on the solenoid. During the release cycle, the

magnetic field was reversed and increased in opposite direction for 10s (35mT) and the magnetic field was removed to let the released particles to be diffused away from the substrate. This cycle was repeatedly applied during the magnetic capture and release ELISA assay. The fluorescence from the magnetic nanoparticles was observed *via* fluorescence microscopy (TE2000U, Nikon, Japan) at a FITC channel (EX 540/25, DM 565, BA605/55, Nikon, Japan).

3.3 Magnetic Capture and Release Cycle

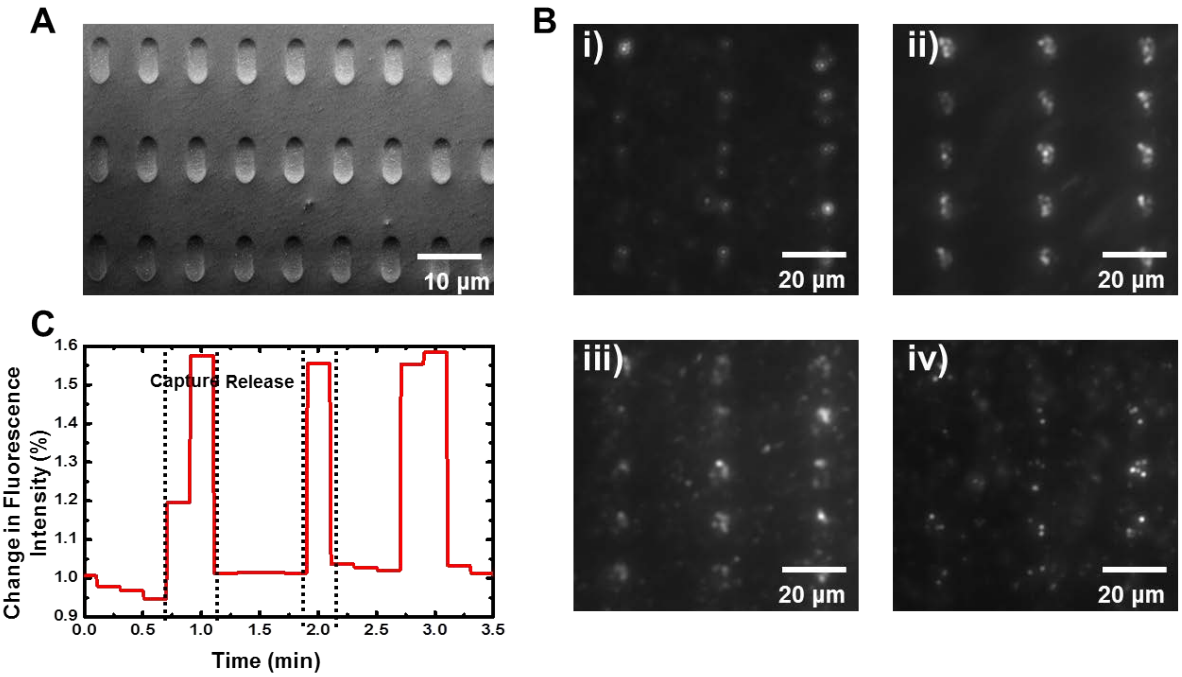

Figure 3.2 Magnetic capture and release cycle. (a) The SEM image of Ni patterns. (b) The fluorescence micrograph of fluorescent magnetic nanoparticles during the magnetic capture and release cycle. i) Absence of magnetic field. ii) Capture cycle. The external magnetic field was applied in perpendicular direction to the plane of the substrate. Magnetic nanoparticles assemble don the Ni patterns. iii) The external magnetic field was removed. Small fractions of magnetic nanoparticles diffuse away from the Ni patterns. iv) Release cycle. The external magnetic field was applied in opposite direction while the local magnetic moment of the Ni patterns remain fixed. The magnetic nanoparticles are released from the Ni patterns.

The figure 3.2b shows fluorescence micrograph of magnetic nanoparticles during the capture and release cycle. In absence of external magnetic field, the magnetic nanoparticles were randomly distributed in the solution (Figure 3.2b i)). When the

external magnetic field was applied in one direction that is perpendicular to the plane of the substrate, the magnetic nanoparticles were drawn towards the Ni patterns on the substrate (Figure 3.2b ii)). Subsequently, when the external magnetic field was reduced to zero, small fraction of magnetic nanoparticles was diffusing away from the Ni patterns (Figure 3.2b iii)). Finally, when the external magnetic field was increased in opposite direction, most of the magnetic nanoparticles were pushed away from the Ni patterns (Figure 3.2b iv)). This phenomenon can be explained as follows; when the external magnetic field was increased in perpendicular direction to the plane of the substrate, the magnetic moment of Ni pattern aligned with the external magnetic field. Therefore, the strength of the magnetic field just above the Ni pattern was stronger than the region without Ni patterns. Since the magnetic nanoparticles move towards the region where the magnetic field is strongest, magnetic nanoparticles assembles on the Ni patterns. When the external magnetic field was removed, the magnetic moments of the Ni patterns remain fixed to the given direction. Therefore, most of the magnetic nanoparticles remained on the Ni patterns and some fraction of magnetic nanoparticles liberated from the Ni pattern by diffusion. When the external magnetic field was increased in opposite direction, the remaining magnetic field of Ni patterns opposed the external magnetic field. Therefore, the magnetic field just above the Ni pattern was weaker than the region without Ni pattern. As a result, the magnetic particles were drawn away from the Ni patterns.

The figure 3.2c shows the fluorescence intensity of the magnetic nanoparticles

as a function of time. The fluorescence intensity was averaged over the Ni patterned region shown in the figure 3.2b. The fluorescence intensity increased rapidly during the capture cycle, but it decreased abruptly during the release cycle. The fluorescence intensity of the magnetic nanoparticles confirms that the magnetic nanoparticles accumulated on the Ni patterned region during the capture cycle, while they are released from the Ni patterned region during the release cycle. It should be noted that, upon the application of external magnetic fields in different directions, magnetic nanoparticles could be repeatedly captured and released from the Ni patterns with short response time.

3.4 Enhancement of the Response Time of ELISA Assay through Magnetic Capture and Release Cycle

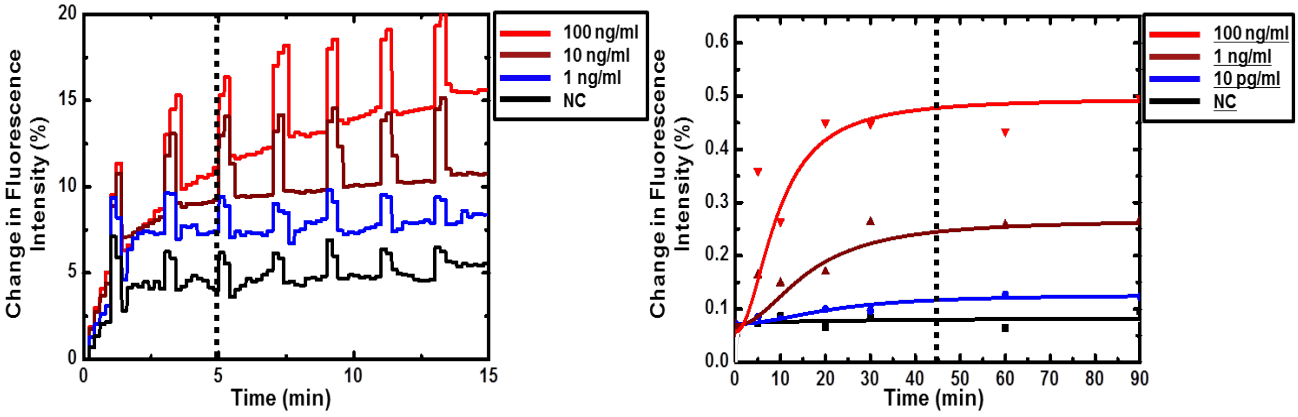

Figure 3.2 Utilization of magnetic capture and release cycle in ELISA assay. (a) Magnetic capture and release ELISA assay. Graph of the fluorescence intensity of the magnetic

nanoparticles with respect to time. (b) Conventional ELISA assay. Graph of the fluorescence intensity of the assay solution with respect to time.

Magnetic capture and release cycle is quite versatile platform which can be utilized for various biosensor device applications for enhancing the response time of the biosensor. Here, we demonstrated magnetic capture and release ELISA assay which exhibits very short response time. We have functionalized the surface of the Ni patterns with primary antibody and the magnetic nanoparticles with secondary antibody as described in chapter 3.2. Then, the flow cell was constructed by covering the antibody labeled substrate with glass slide and the 3M double sided tape was used as a spacer. The assay solution containing antibody-labeled superparamagnetic nanoparticles (1.8×10^{11} unit/ml) mixed with the target antigen (100 ng/ml, 10 ng/ml and 1 ng/ml of IL-13 for the positive control and 1 ng/ml of IL-4 for negative control) was injected into the flow cell and placed on top of custom-built solenoid. The capture and release cycle was repeatedly applied during the magnetic capture and release ELISA assay.

The figure 3.3a shows the change in fluorescence intensity of magnetic nanoparticles on the Ni patterned region. The crests in the fluorescence intensity profile correspond to the capture cycle, while the troughs correspond to the release cycle. When the magnetic capture and release cycle was repeatedly applied, the fluorescence intensity of magnetic particle for all different concentration of target antigen starts to increase. However, it is apparent that the fluorescence intensity of the assay solution with higher target concentration increased at much faster rate and reached higher maximum

fluorescence intensity, whereas that with lower target concentration or the non-complementary target increased at much slower rate and reached lower maximum fluorescence intensity. For all assay solution with different antigen concentration, the change in the fluorescence intensity leveled off after 5 minute. The magnetic nanoparticles were repeatedly drawn and pushed away from the Ni patterns during the magnetic capture and release cycle. However, when the secondary antibodies functionalized on the magnetic nanoparticles happen to capture the antigen molecules floating in the solution and drawn towards the primary antibody immobilized on the Ni patterns, antigen-antibody interaction was formed which immobilized the magnetic nanoparticles on the Ni patterns. During the release cycle, the magnetic nanoparticles with free secondary antibodies were pushed away from the Ni patterns due to the magnetic field gradient, whereas the magnetic particle with antigen bound secondary antibodies remained on the Ni pattern due to the antigen-antibody interaction. These immobilized magnetic nanoparticles resulted in the increase in the fluorescence intensity of the Ni patterned region. When the concentration of the target antigen in the assay solution is high, it is more likely for the secondary antibodies to capture the target antigen and hence more fractions of fluorescent magnetic particles become immobilized on the Ni patterned region. This results the higher maximal fluorescence intensity of the assay solution with higher target antigen concentration. However, when the concentration of the target antigen in the assay solution is low, it is less likely for the secondary antibodies to capture the target antigen and hence smaller fractions of fluorescent magnetic particles become immobilized on the Ni patterned region. This results the lower maximal

fluorescence intensity of the assay solution with lower target antigen concentration. Finally, if there is no complementary antigen molecule present in the assay solution (NC of the figure 3.3a), none of magnetic nanoparticles should be fixed on the Ni patterned region due to the antigen-antibody interaction. It should be noted that the slight increase in the fluorescence intensity of the assay solution containing non-complementary antigen result from the non-specific adsorption of magnetic nanoparticles to the Ni patterned substrate. [62] This result indicates that the utilization of magnetic capure and release cycle in ELISA assay allows detection of target antigen within very short time window.

We have also performed a conventional ELISA assay on our Ni patterned substrate and measured the response time (figure 3.3b). Here, we have placed assay solution with different concentration of antigen on the Ni patterned substrate and incubate for given time intervals (0 min, 5 min, 10min, 20min, 30 min, 60 min and 90 min). After the incubation, the substrate was rinsed with PBS buffer for 3 times and dried with N_2 blow gun. Then, the each substrate was incubated with secondary antibody for 2 hr and washed with PBS buffer. Subsequently, the substrate was incubated in streptavidin labeled horse radish peroxidase solution for 30 min and washed with PBS buffer. Afterward, the substrate was incubated in 3,3',5,5'-tetramethylbenzidine (TMB) solution and let to react for 15 min. Finally, the stop solution composed of 1M phosphoric acid was added to stop the reaction and the absorbance of the assay solution was obtained using microplate reader. The result indicates that, for all assay solution with different antigen concentration, the change in fluorescence intensity reaches its maximum

approximately after 45 min of the incubation which was 9 times longer than the magnetic capture and release ELISA assay. It should be also noted that the magnetic capture and release ELISA assay does not require any further incubation and washing steps after the magnetic capture and release step, whereas conventional ELISA assay requires additional several hours of incubation and washing steps before the data acquisition. This result indicated that the utilization of magnetic capture and release cycle in ELISA assay reduces the detection time significantly.

3.5 Summary

In conclusion, we report the magnetic capture and release cycle which can repeatedly capture and release the superparamagnetic nanoparticles to the predetermined Ni patterned regions and their application in the ELISA assay to reduce the detection time. Our magnetic capture and release system utilizes superparamagnetic particles functionalized with secondary antibodies which captures the target antigen floating in the solution, and the Ni patterns functionalized with primary antibody which recognizes the target antigen brought by the secondary antibodies of the superparamagnetic nanoparticles. We have demonstrated that repeated application magnetic capture and release cycle allowed the accumulation of the magnetic nanoparticles that have captured the target antigens on the Ni patterned region, whereas the magnetic nanoparticles without captured target antigens were repeatedly captured and released from the Ni

patterned region until they captures the free antigens in the solution. These results clearly shows that the application of the magnetic capture and release cycle in biomolecular detection greatly reduces the time required for the detection of biomolecules. Since our strategy provides a means to reduce the detection time significantly, it should open up various applications such as development of ultra-fast biosensors and cargo delivery in biochip. [17]

Chapter 4.

Conclusions

In this dissertation, first, we discussed a fabrication strategy of NSW structures which can be deposited onto virtually-general substrates to build nano-storage devices for the real-time controlled release of biochemical molecules upon the application of electrical stimuli. The NSWs were composed of three different segments comprised of a polypyrrole (PPy) segment containing chemical species such as ATP, a ferromagnetic nickel (Ni) segment, and a conductive gold (Au) segment. respectively. NSWs have been deposited onto specific locations on solid substrates *via* various methods such as direct writing or magnetic field driven assembly, and they were utilized for the controlled release of ATP. We also demonstrated the deposition of NSWs onto *flexible substrates* or *the end of micropipettes* to fabricate *flexible* or *probe-type* nano-storage devices, respectively. These results clearly show that NSWs are quite versatile structures allowing us to fabricate nano-storage devices on virtually general substrates for the controlled release of biochemical molecules. Thus, our strategy should provide great opportunities in various areas such as drug delivery systems [18-21] biosensors [15,16] and biochips [13] for the controlled release of chemicals to bio-systems

Secondly, we have developed the magnetic capture and release cycle which can repeatedly capture and release the superparamagnetic nanoparticles to the predetermined Ni patterned regions. Additionally, this system was utilized in the ELISA assay to reduce

the detection time. Our magnetic capture and release system utilizes superparamagnetic particles functionalized with secondary antibodies which captures the target antigen floating in the solution, and the Ni patterns functionalized with primary antibody which recognizes the target antigen brought by the secondary antibodies of the superparamagnetic nanoparticles. We have demonstrated that the repeated application magnetic capture and release cycle allowed the accumulation of the magnetic nanoparticles that have captured the target antigens on the Ni patterned region, whereas the magnetic nanoparticles without captured target antigens were repeatedly captured and released from the Ni patterned region until they captures the free antigens in the solution. These results clearly shows that the application of the magnetic capture and release cycle in biomolecular detection greatly reduces the time required for the detection of biomolecules. Since our strategy provides a means to reduce the detection time significantly, it should open up various applications such as development of ultra-fast biosensors and cargo delivery in biochip.

In conclusion, we have developed a technologies to activity control the biomolecules and delivery of chemical and biological molecules through the utilization of electric and magnetic control of nanostructures. These works should strongly contribute to the mass transport of specific chemical species and the controlled activation of biomolecules in drug delivery systems [18-21] biosensors [15,16] and biochips. [13]

Chapter 5.

References

1. Vo-Dinh, Y.; Cullum, B., Biosensors and Biochips: Advances in Biological and Medical Diagnostics, *Fresenius J Anal Chem*, **2000,** 366, 540–551.
2. Meyer, M.; Wilson, P.; Schomburg, D., Hydrogen Bonding and Molecular Surface Shape Complementarity as a Basis for Protein Docking, *J. Mol. Biol*, **1996,** 264, 199–210.
3. Ghoshal, S.; Mitra, D.; Roy, S.; Dutta-Majumder, D., Biosensors and Biochips for Nanomedical Applications: a Review, *Sensors & Transducers Journal*, **2011,** 113, 1-17.
4. Dwyer, M.; Hellinga, H., Periplasmic Binding Proteins: a Versatile Superfamily for Protein Engineering, *Curr. Opin. Struct. Biol*, **2004,** 14, 495–504.
5. Homola, J.; Yee, S.; Gauglitz, G., Surface Plasmon Resonance Sensors: Review, *Sens. Actuators, B,* **1999,** 54, 3–15.
6. Jacobs, C.; Peairs, J.; Venton, j., Review: Carbon Nanotube Based Electrochemical Sensors for Biomolecules, *Anal. Chim. Acta*, **2010**, 662, 105–127.
7. Jianrong, C.; Yuqing, M.; Nongyue , H.; Xiaohua, W.; Sijiao, L., Nanotechnology and Biosensors, *Biotechnol. Adv*, **2004**, 22, 505–518.
8. Bangar, M. A.; Hangarter, C. M.; Yoo, B.; Rheem, Y.; Chen, W.; Mulchandani,

A.; Myung, N. V., Magnetically Assembled Multisegmented Nanowires and Their Applications. *Electroanal.* **2009,** *21*, 61-67.

9. Garcia-Gradilla, V.; Orozco, J.; Sattayasamitsathit, S.; Soto, F.; Kuralay, F.; Pourazary, A.; Katzenberg, A.; Gao, W.; Shen, Y.; Wang, J., Functionalized Ultrasound-Propelled Magnetically Guided Nanomotors: Toward Practical Biomedical Applications, *ACS nano*, **2013**, 7, 9232–9240.
10. Koh, I.; Hong, R.; Weissleder, R.; Josephson, L., Sensitive NMR Sensors Detect Antibodies To Influenza, *Angew Chem Int Ed Engl*. **2008,** 47, 4119–4121.
11. Bray, D., Protein Molecules as Computational Elements in Living Cells. *Nature* **1995,** *378*, 419-419.
12. Spudich, J. A., How Molecular Motors Work. *Nature* **1994,** *372*, 515-518.
13. Sundberg, M.; Bunk, R.; Albet-Torres, N.; Kvennefors, A.; Persson, F.; Montelius, L.; Nicholls, I. A.; Ghatnekar-Nilsson, S.; Omling, P.; Tagerud, S.; et al., Actin Filament Guidance on a Chip: Toward High-Throughput Assays and Lab-on-a-Chip Applications. *Langmuir* **2006,** *22*, 7286-7295.
14. Mir, M.; Homs, A.; Samitier, J., Integrated Electrochemical DNA Biosensors for Lab-on-a-Chip Devices. *Electrophoresis* **2009,** *30*, 3386-3397.
15. Jin, H. J.; Lee, S. H.; Kim, T. H.; Park, J.; Song, H. S.; Park, T. H.; Hong, S., Nanovesicle-based Bioelectronic Nose Platform Mimicking Human Olfactory Signal Transduction. *Biosens. Bioelectron.* **2012,** *35*, 335-341.
16. Lee, B. Y.; Seo, S. M.; Lee, D. J.; Lee, M.; Lee, J.; Cheon, J. H.; Cho, E.; Lee, H.; Chung, I. Y.; Park, Y. J.;et al, Biosensor System-on-a-Chip Including CMOS-

based Signal Processing Circuits and 64 Carbon Nanotube-based Sensors for the Detection of a Neurotransmitter. *Lab Chip* **2010,** *10*, 894-898.

17. Sheehan, P.; Whitman, L., Detection Limits for Nanoscale Biosensors, *Nano Lett,* **2005,** 5, 803-807
18. Tao, S. L.; Desai, T. A., Microfabricated Drug Delivery Systems: from Particles to Pores. *Adv. Drug Deliver. Rev.* **2003,** *55*, 315-328.
19. George, P. M.; LaVan, D. A.; Burdick, J. A.; Chen, C. Y.; Liang, E.; Langer, R., Electrically Controlled Drug Delivery from Biotin-Doped Conductive Polypyrrole. *Adv. Mater.* **2006,** *18*, 577-581.
20. Geetha, S.; Rao, C. R. K.; Vijayan, M.; Trivedi, D. C., Biosensing and Drug Delivery by Polypyrrole. *Anal. Chim. Acta.* **2006,** *568*, 119-125.
21. Ge, D. T.; Tian, X. D.; Qi, R.; Huang, S. Q.; Mu, J.; Hong, S. M.; Ye, S. F.; Zhang, X. M.; Li, D. H.; Shi, W., A Polypyrrole-based Microchip for Controlled Drug Release. *Electrochim. Acta.* **2009,** *55*, 271-275.
22. Santini, J. T.; Richards, A. C.; Scheidt, R.; Cima, M. J.; Langer, R., Microchips as Controlled Drug-Delivery Devices. *Angew. Chem. Int. Edit.* **2000,** *39*, 2397-2407.
23. Razzacki, S. Z.; Thwar, P. K.; Yang, M.; Ugaz, V. M.; Burns, M. A., Integrated Microsystems for Controlled Drug Delivery. *Adv. Drug Deliver. Rev.* **2004,** *56*, 185-198.
24. Saltzman, W. M.; Olbricht, W. L., Building Drug Delivery into Tissue Engineering. *Nat. Rev. Drug Discov.* **2002,** *1*, 177-186.

25. Goldman, E. W.; Hibberd, M.G.; McCray J.A.; Trentham, D.R., Releaxation of Muscle Fibers by Photolysis of Caged ATP. *Nature*. **1982**, 300, 701-705.

26. Goldman, E. W.; Hibberd, M.G.; Trentham, D.R., Relaxation of Rabbit Psoas Muscle Fibres from Rigor by Photochemical Generation of Adenosine-5'-Triphosphate. *J. Physiol*. **1984**. 354, 577-604.

27. Dantzig, J. A.; Goldman, Y. E.; Millar, N. C.; Lacktis, J.; Homsher, E., Reversal of the Cross-Bridge Force-Generating Transition by Photogeneration of Phosphate in Rabbit Psoas Muscle Fibers. *J. Physiol*. **1992**. 451, 247-278.

28. Goldman, Y. E,; Hibberd, M. G.; Trentham, D.R., Relaxation of Rabbit Psoas Muscle Fibres from Rigor by Photochemical Generation of Adenosine-5'-Triphosphate. *J. Physiol*. **1984**. 354, 577–604.

29. Hess, H.; Clemmens, J.; Qin, D.; Howard, J.; Vogel, V. Light- Controlled Molecular Shuttles Made from Motor Proteins Carrying Cargo on Engineered Surfaces. *Nano Lett*. **2001**, 1, 235–239.

30. Grove, T. J; Puckett, K. A.; Brunet, N. M.; Mihajlovic, M.; McFadden, L. A.; Xiong, P.; von Molnar, S.; Moerland, T. S.; Chase, P. B., Packaging Actomyosin-based Biomolecular Motor-Driven Devices for Nanoactuator Applications. *IEEE Trans. Adv. Packag*, 2005, 28, 556-563.

31. Paciotti, G. F.; Kingston, D. G. I.; Tamarkin, L., Colloidal Gold Nanoparticles: A Novel Nanoparticle Platform for Developing Multifunctional Tumor-Targeted Drug Delivery Vectors. *Drug Develop. Res.* **2006,** *67*, 47-54.

32. Gelperina, S.; Kisich, K.; Iseman, M. D.; Heifets, L., The Potential Advantages of Nanoparticle Drug Delivery Systems in Chemotherapy of Tuberculosis. *Am. J. Resp. Crit. Care.* **2005,** *172*, 1487-1490.

33. Paciotti, G. F.; Myer, L.; Weinreich, D.; Goia, D.; Pavel, N.; McLaughlin, R. E.; Tamarkin, L., Colloidal gold: A Novel Nanoparticle Vector for Tumor Directed Drug Delivery. *Drug Deliv.* **2004,** *11*, 169-183.

34. Sharma, H. S.; Ali, S. F.; Dong, W.; Tian, Z. R.; Patnaik, R.; Patnaik, S.; Sharma, A.; Boman, A.; Lek, P.; Seifert, E.; Lundstedt, T., Drug Delivery to the Spinal Cord Tagged with Nanowire Enhances Neuroprotective Efficacy and Functional Recovery Following Trauma to the Rat Spinal Cord. *Ann. N.Y. Acad. Sci.* **2007,** *1122*, 197-218.

35. Fischer, K. E.; Aleman, B. J.; Tao, S. L.; Daniels, R. H.; Li, E. M.; Bunger, M. D.; Nagaraj, G.; Singh, P.; Zettl, A.; Desai, T. A., Biomimetic Nanowire Coatings for Next Generation Adhesive Drug Delivery Systems. *Nano Lett.* **2009,** *9*, 716-720.

36. Fan, Z. Y.; Ho, J. C.; Takahashi, T.; Yerushalmi, R.; Takei, K.; Ford, A. C.; Chueh, Y. L.; Javey, A., Toward the Development of Printable Nanowire Electronics and Sensors. *Adv. Mater.* **2009,** *21*, 3730-3743.

37. Fan, Z. Y.; Ho, J. C.; Jacobson, Z. A.; Yerushalmi, R.; Alley, R. L.; Razavi, H.; Javey, A., Wafer-Scale Assembly of Highly Ordered Semiconductor Nanowire Arrays by Contact Printing. *Nano Lett.* **2008,** *8*, 20-25.

38. Bangar, M. A.; Hangarter, C. M.; Yoo, B.; Rheem, Y.; Chen, W.; Mulchandani, A.; Myung, N. V., Magnetically Assembled Multisegmented Nanowires and

Their Applications. *Electroanal.* **2009,** *21*, 61-67.

39. Wanekaya, A. K.; Chen, W.; Myung, N. V.; Mulchandani, A., Nanowire-based Electrochemical Biosensors. *Electroanal.* **2006,** *18*, 533-550.
40. Kovtyukhova, N. I.; Mallouk, T. E., Nanowires as Building Blocks for Self-Assembling Logic and Memory Circuits. *Chem-Eur. J.* **2002,** *8*, 4355-4363.
41. Qin, L. D.; Park, S.; Huang, L.; Mirkin, C. A., On-Wire Lithography. *Science* **2005,** *309*, 113-115.
42. Byun, K. E.; Choi, D. S.; Kim, E.; Seo, D. H.; Yang, H.; Seo, S.; Hong, S., Graphene-Polymer Hybrid Nanostructure-Based Bioenergy Storage Device for Real-Time Control of Biological Motor Activity. *ACS Nano.* **2011,** *5*, 8656-8664.
43. Pernaut, J. M.; Reynolds, J. R., Use of Conducting Electroactive Polymers for Drug Delivery and Sensing of Bioactive Molecules. A Redox Chemistry Approach. *J. Phys. Chem. B* **2000,** *104*, 4080-4090.
44. Xiao, Y. H.; Che, J. F.; Li, C. M.; Sun, C. Q.; Chua, Y. T.; Lee, V. S.; Luong, J. H. T., Preparation of Nano-Tentacle Polypyrrole with Pseudo-Molecular Template for ATP Incorporation. *J. Biomed. Mater. Res. A.* **2007,** *80A*, 925-931
45. Lee, B. Y.; Heo, K.; Schmucker, A. L.; Jin, H. J.; Lim, J. K.; Kim, T.; Lee, H.; Jeon, K. S.; Suh, Y. D.; Mirkin, C. A.; et al., Nanotube-Bridged Wires with Sub-10 nm Gaps. *Nano Lett.* **2012,** *12*, 1879-1884
46. Böhm, K. J.; Stracke, R.; Baum, M.; Zieren, M.; Unger, E., Effect of Temperature on Kinesin-Driven Microtubule Gliding and Kinesin ATPase Activity. **2000**, *FEBS lett*, 46, 59-62

47. van den Heuvel, M. G. L.; Butcher, C. T.; Lemay, S. G.; Diez, S.; Dekker, C., Electrical Docking of Microtubules for Kinesin-Driven Motility in Nanostructures. *Nano Lett*. **2005**, 5, 235-241.

48. Tanase, M.; Silevitch, D. M.; Hultgren, A; Bauer, L. A.; Searson, P. C.; Meyer, G. J.; Reich, D. H., Magnetic Trapping and Self-Assembly of Multicomponent Nanowires. *J. Appl. Phys.* **2002**, 91, 8549-8551.

49. Ye, H.; Gu, Z.; Y, T.; Gracias, D. H., Integrating Nanowires with Substrates Using Directed Assembly and Nanoscale Soldering. *IEEE Trans. Nanotechnol*. **2006**, 5, 62-66.

50. Critchley, Kevin; Khanal, Bishnu P.; Górzny, Marcin Ł.; Vigderman, Leonid; Evans, Stephen D.; Zubarev, Eugene R.; Kotov, Nicholas A., Near-Bulk Conductivity of Gold Nanowires as Nanoscale Interconnects and the Role of Atomically Smooth Interface. *Adv. Mater.* **2010**, 22, 2338-2342.

51. Williams, K. R.; Gupta, K.; Wasilik, M., Etch Rates for Micromachining Processing - Part II. *J. Microelectromech. S.* **2003,** *12*, 761-778.

52. Lopez Cascales, J.J.; Otero, T. F., Molecular Dynamic Simulation of the Hydration and Diffusion of Chloride Ions from Bulk Water to Polypyrrole Matrix. *J. Chem. Phys*. **2004**, 120, 1951-1957.

53. Lopez Cascales, J.J.; Fernandez, A. J.; Otero, T. F., Characterization of the Reduced and Oxidized Polypyrrole/Water Interface: a Molecular Dynamics Simulation Study. *J. Phys. Chem. B.* **2003**, 107, 9339-9343.

54. Siepmann, J.; Ainaoui, A.; Vergnaud, J. M.; Bodmeier, R. Calculation of the

Dimensions of Drug-Polymer Devices Based on Diffusion Parameters. J. Pharm. Sci. **1998**, 87, 827-832.

55. Nomura, A.; Uyeda, T. Q. P.; Yumoto, N.; Tatsu, Y. Photo- Control of Kinesin-Microtubule Motility Using Caged Peptides Derived from the Kinesin C-Terminus Domain. *Chem. Commun*. **2006**, 3588–3590.
56. Mihajlovic, G.; Brunet, N. M.; Trbovic, J.; Xiong, P.; Von Molnar, S.; Chase, P. B. All-Electrical Switching and Control Mechanism for Actomyosin-Powered Nanoactuators. *Appl. Phys. Lett*. **2004**, 85, 1060–1062.
57. Ionov, L.; Stamm, M.; Diex, S., Reversible Switching of Microtubule Motility Using Thermosensitive Polymer Surfaces. *Nano Lett*. **2006**, 6, 1982-1987.
58. Son, D.; Park, S. Y.; Kim, B.; Koh, J. T.; Kim, T. H.; An, S.; Jang, D.; Kim, G. T.; Jhe, W.; Hong, S., Nanoneedle Transistor-Based Sensors for the Selective Detection of Intracellular Calcium Ions. *ACS Nano.* **2011,** *5*, 3888-3895.
59. Heller, M.; Forster, A.; Tu, E., Active Microelectronic Chip Devices which Utilizes Controlled Electrophoretic Field for Multiplex DNA Hybridization and Other Genomic Applications, *Electrophoresis*, **2000**, 21, 157-164
60. Bhatia, S.; Shriver-Lake, L.; Prior, K.; Georger, J.; Calvert, J.; Bredehorst, R.; Ligle, F., Use of Thiol-Terminal Silanes and Heterobifunctional Crosslinkers for Immobilization of Antibodies on Silica Surfaces, *Anal. Biochem*,**1989,** 178, 408-413.
61. Taylor, J.; Fang, M.; Nie, S., Probing Specific Sequences on Single DNA Molecules with Bioconjugated Fluorescent Nanoparticles, Anal. Chem. **2000**, 72,

1979-1986.

62. Aytur, T.; Foley, J.; Anwar, M.; Boser, B.; Harris, E.; Beatty, P., A Novel Magnetic Bead Bioassay Platform using a Microchip-based Sensor for Infectious Disease Diagnosis, *J. Immunol. Methods*, **2006,** 314, 21–29.

Chapter 6.

Abstract in Korean

초록

나노구조체의 전기적 자기적 조절과 이를 이용한 바이오칩 분야의 응용에 관한 연구

이동준

생물물리 및 화학 생물학부

서울대학교 대학원

본 연구에서는 전기적 및 자기적 자극을 통한 나노구조의 조절에 관한 연구 및 이를 이용한 바이오 칩 개발에서의 응용에 관한 연구를 진행하였다. 먼저, 화학물질을 저장하고 외부 전기 자극을 통해 원하는 순간에 화학물질을 방출할 수 있는 "화학물질 저장 나노선"(nano-storage wire)을 개발하였다. 양극처리 된 알루미늄 산화물 템플릿에 전기 도금 법을 이용하여 Adenosine triphosphate (ATP)분자를 저장하고 방출할 수 있는 전도성 중합체인 Polypyrrole 부분, 강자성 니켈 부분 및 높은 전도성 가지는 금 부분 등으로 구성된 다중구조 나노선을 제조하였다. 이러한 화학물질 저장 나노선에 전압을 인가하면 화학물질 저장 나노선의 Polypyrrole 부분으로부터 ATP 분자가 방출되게 되어 모터 단백질의 기능을 조절할 수 있다. 또한, 화학물질 저장 나노선을 포함한 용액을 잉크처럼 사용하거나 자가조립 기법을 이용하여 다양한 3차원 구조의 기판 위에 인쇄를 함으로서 다목적 화학물질 저장소자를 제작할 수 있다. 본 기술은 화학물질을 저장 하고 선택적으로 방출할 수 있는 소자를 제작할 수 있기 때문에 약물 전달 시스템 및 바이오 칩 등의 실질적인

응용에 기여할 것이다.

또한, 자기적 포집 및 방출 사이클의 응용을 통해 초고속 효소결합면역흡착 검사를 개발하였다. 자기적 포집 및 방출 사이클은 크게 두 가지 구성요소로 구성되어 있는데 일차 항체로 기능화된 니켈의 패턴 어레이와 이차 항체로 기능화된 초상자성 나노입자가 그것이다. 자기적 포집 및 방출 사이클을 반복적으로 인가 해주면, 초상자성 나노입자들이 니켈 패턴 어레이에 능동적으로 포집되 거나 방출되게 된다. 이때, 초상자성 나노입자에 기능화된 항체가 검지 용액 내에 존재 하는 타겟 항원과 반응 하고 이를 니켈 패턴 어레이로 운송을 하게되면, 일차 항체-항원-이차 항체 간의 결합이 형성하게 되어 초상자성 나노입자들을 니켈 패턴 표면에 고정시키게 된다. 이 메커니즘을 통하여 검지 용액 내에 존재하는 항원을 5분이내에 검출할 수 있는 시스템을 개발하였다. 이 기술은 검출 시간에 필요한 시간을 크게 단축 하며 특정물질을 원하는 위치로 수송할 수 있으므로 초고속 바이오 센서의 개발 및 바이오 칩 내부에서의 물질수송 등의 다양한 응용 분야에 활용 될 수 있을 것이다.

주요어: 나노선, 전도성 중합체, 폴리파이롤, 선택적 방출, 바이오에너지 저장, 나노바이오 인터페이스, 초상자성 나노입자, 감지시간, 효소결합면역흡착검사, 자디적 포집 및 방출 사이클, 바이오 칩.

학번: 2012-22515